ABTIN: ABsolute TIssue density from NODDI, focusing on myelin density

Farshid Sepehrband[1,2], Kristi A Clark[3], Jeremy F. P Ullmann[1], Nyoman D Kurniawan[1], Gayeshika Leanage[1], David C Reutens[1], and Zhengyi Yang[1,4]
[1]*Centre for Advanced Imaging, University of Queensland, Brisbane, Queensland, Australia,* [2]*Queensland Brain Institute, University of Queensland, Brisbane, Queensland, Australia,* [3]*Institute for Neuroimaging and Informatics, University of Southern California, Los Angeles, California, United States,* [4]*School of Information Technology and Electrical Engineering, University of Queensland, Brisbane, Queensland, Australia*

Target audience: This abstract is intended for quantitative and microstructural imaging communities.

Purpose: Recently, modeling techniques have used Diffusion Weighted Imaging (DWI) to infer specific tissue characteristics such as neurite density and dispersion[1,2]. However, these techniques only yield relative measurements of tissue compartment density because they are insensitive to compartments with low water concentration, such as myelin, which comprises 70% lipid and 30% protein[3]. More recently, the NODDI technique[2] and quantitative magnetization transfer have been used to measure the g-ratio (the ratio between axon and fiber diameter) across the whole brain[4,5]. The g-ratio remained relatively constant across the whole brain at ~0.6-0.8, corroborating previous findings. In this study, we propose a method (ABTIN) exploiting prior knowledge about myelin and cell membrane contributions to obtain absolute tissue density from relative tissue density measured with the NODDI method. Specifically, we used a fixed g-ratio to relate the axon volume fraction to the myelin volume fraction. We also defined a parameter that relates the cell volume fraction to the cell membranes. We tested our method with *ex vivo* imaging of a mouse brain and validated the measures using electron microscopy (EM) analysis across sub-regions of the corpus callosum (CC).

Methods:

Theory: To define the fraction occupied by the absolute volume of each tissue compartment, tissue components that do not contribute to the diffusion signal, such as myelin and cell membranes must be included. Extending the compartment model used in NODDI, we define the absolute volume of brain tissue as the combination of volumes representing neurites (V_n), cells (V_c), cerebrospinal fluid (V_{csf}) and tissue compartments that experience no signal attenuation from diffusion weighting (myelin (V_m) and membranes of cells and cellular processes (V_{cm})). Hence, $F_{in} = V_n / (1-V_m-V_{cm})$, $F_{en} = V_c / (1-V_m-V_{cm})$, $F_{csf} = V_{csf} / (1-V_m-V_{cm})$ (F_{in}, F_{en}, F_{csf}: intra-neurite, extra-neurite and CSF volume fraction),

where F_{in}, F_{en} and F_{csf} represent the volume fractions of the diffusion signal, originating from V_n, V_c and V_{csf}, respectively. Because V_m and V_{cm} represent compartments that do not contribute significantly to the diffusion signal, assumptions based on prior knowledge are required to link NODDI volume fraction measures (F_{in}, F_{en} and F_{csf}) with tissue density. The relationship between axonal and myelin density is obtained by fixing the g-ratio (g), and can be defined as: $V_m = (g^{-2} - 1)\, V_n$. In addition, we assumed a linear relationship between cell density and cell membrane density ($V_c = \alpha V_{cm}$), setting α at 25. The membranes of cells, dendrites and axons are thin, ranging from 3 to 10 nm [6], and represent 1 to 4% of the cell volume [7], corresponding to α of at least 25.

Preparation and DWI: An adult mouse (C57BL/6J) was fixed and imaged on a 16.4 T Bruker scanner (Bruker Biospin, Germany) using a 15 mm SAW coil (M2M Imaging, USA). Three mid-sagittal slices were scanned with in plane resolution of 100×100 µm and slice thickness of 300 µm (only the most central slice was used). G_{max} of 1.3 T/m: 4 shells, each with 60 gradient directions (obtained from Camino[8]), G = {1107, 1227, 464, 509} mT/m, δ = {1.1, 2.3, 6.3, 5.6} ms, Δ = {28.4, 7.0, 23.0, 23.7} ms, TE/TR of 35/750 ms was used.

EM imaging: Following imaging, the brain was sectioned sagittally at 50µm thickness using a vibratome. On the mid-sagittal section, the CC was isolated and samples of the genu, body and splenium were separated. Sample preparation was carried out according to the methods described in [10]. Sections were cut on a UC6 ultra-microtome (ultracut S, Reichert, Leica, Sweden) at 60nm, and imaged at ×5000 in a transmission electron microscope at 80 kV (JEM 1011, Jeol, Japan). Images were captured with an Olympus Morada digital camera. For each region of the CC, two images, with FOV of around 50×50 µm were acquired. Myelin were segmented using random forest classification. Each segmented EM image was divided into 100 windows of 5×5 µm and the myelin density was then calculated for each window (An example is presented in Fig. 1B).

Data analysis: For each voxel of the multi-shell data, the NODDI tissue model was fitted to the data to obtain estimates of F_{in}, F_{en} and F_{csf}. An extra compartment was used to model stationary water in an *ex vivo* experiment, as suggested in [9]. Tissue compartment densities (V_n, V_m, V_c, V_{cm}, and V_{csf}) were obtained by numerically solving above equations. The mean value of the estimated g-ratio from EM analysis (g-ratio = 0.7) was used. Estimated myelin density was compared with that from EM. For each dataset (EM and myelin density map), one-way ANOVA (Analysis of variance) was performed to evaluate mean differences across sub-regions of the CC. When comparing across datasets two-sample t-test was employed.

Results:

In the regions of interest, myelin density values obtained from ABTIN were comparable with those obtained from EM (Fig. 1C). Mean myelin density from ABTIN and the EM images were not significantly different (p = 0.63, 0.76, and 0.5, for the genu, body and splenium of the CC, respectively). As with the EM analysis, a high-low-high trend was observed for genu-body-splenium. In both EM and ABTIN, myelin density in splenium and genu were significantly higher than in the body ($p < 0.01$). In the whole mid-sagittal slice, the highest myelin density values (from ABTIN) were observed in the CC and the thalamus (Fig. 1A). Ignoring cerebrospinal fluid regions, where myelin density is almost zero, the lowest estimated myelin density values were in gray matter. Cell density varied inversely with myelin density (Fig. 1D).

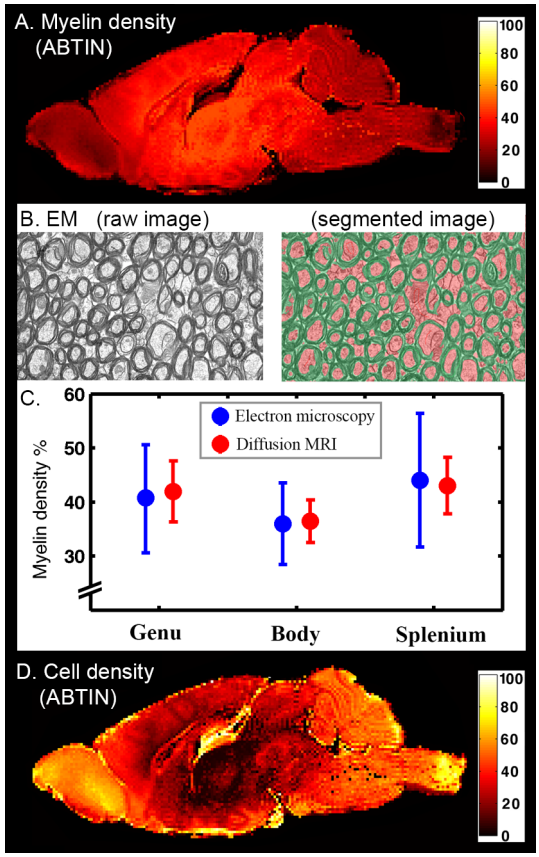

Figure 1. (A) Myelin density form ABTIN, (B) An example of myelin segmentation from EM (accurate segmentation was obtained using random forest classification, having out-of-bag error of < 1% and a precision and recall of ~1), (C) Mean and S.D. of myelin density values from EM and ABTIN, across sub-regions of the CC. (D) Cell density from ABTIN.

Discussion and Conclusion:

We describe a method to obtain absolute tissue density directly from DWI. We found a significant correlation between ABTIN myelin density measures and those obtained from EM in the mouse CC. In contrast to previous techniques that can only infer relative values, or require additional modalities, ABTIN is the first technique, which can calculate measurements of absolute tissue density directly from DWI. ABTIN would be beneficial in studies of neurological diseases or neurodevelopment where changes in axon are suspected to be the most informative e.g. axonal guidance or axonal loss, but not in demyelination (the fixed value for the g-ratio render the technique insensitive to demyelination).

Acknowledge: We would like to thank Prof. D. Alexander for his valuable inputs.

References:

1) H. Zhang, et al., 2012, Neuroimag 61, 1000–1016.
2) S.N. Jespersen, et al., 2010, Neuroimage 49, 205–216.
3) N. Baumann, et al., 2001, Physiological Reviews 81, 871–927.
4) J. Campbell, et al., 2013, ISMRM workshop on microstructural imaging.
5) N. Stikov, et al., 2014, ISMRM 22th, 0102.
6) A.Chen, et al., 2000, Biophysical Journal 78, 2814–2820.
7) C.V. Howard, et al, 1993, Neuroprotocols 2, 113–120.
8) P. Cook, et al., 2007, JMRI 25, 1051–1058.
9) D. C. Alexander, et al., 2010, Neuroimage, 52, 1–16.
10) S.A. Wilke, et al., 2013, Journal of Neuroscience, 33, 507–22.